

Original Article

# Activation of fibroblasts by plasma cells via PDGF/PDGFR signaling in IgG4-related sialadenitis

Takumi Kitaoka,<sup>1)</sup> Rintaro Ohe,<sup>1)</sup> Takanobu Kabasawa,<sup>1)</sup> Masayuki Kaneko,<sup>1,2)</sup>

Nobuyuki Sasahara,<sup>1,3)</sup> Michihisa Kono,<sup>1)</sup> Kazushi Suzuki,<sup>1)</sup> Naoya Uchiyama,<sup>1)</sup> Rinako Ogawa,<sup>1)</sup>

Mitsuru Futakuchi<sup>1)</sup>

IgG4-related sialadenitis (IgG4-SA) is one of the IgG4-related disease. The histological features of IgG4-SA include dense lymphoplasmacytic infiltrates and fibrosis. This study aimed to reveal the involvement of plasma cells in the development of fibrosis and the mechanism underlying fibrosis in IgG4-SA. Hematoxylin-eosin staining, Azan staining, silver staining, and immunohistochemistry (IHC) were performed on IgG4-SA and chronic sialadenitis specimens, and these samples were analyzed by image analysis software. Histological spatial analysis was used to analyze the localization of IHC-positive cells and the distances between these cells. In the IgG4-SA group, many secondary lymphoid follicles with germinal centers were found, and many collagen fibers developed around these germinal centers. Collagen fibers composed mainly of type I collagen was abundant at sites away from secondary lymphoid follicles, and reticular fibers composed of type III collagen was abundant near secondary lymphoid follicles. Many FAP<sup>+</sup> fibroblasts and MUM1<sup>+</sup> plasma cells were localized near secondary lymphoid follicles. Histological spatial analysis demonstrated that 90.4% of MUM1<sup>+</sup> plasma cells accumulated within 20  $\mu$ m of FAP<sup>+</sup> fibroblasts. Multiple immunofluorescence assays revealed that MUM1<sup>+</sup> plasma cells expressed platelet-derived growth factor (PDGF)  $\beta$ , and FAP<sup>+</sup> fibroblasts expressed PDGF receptor (PDGFR)  $\beta$  and pSTAT3 in IgG4-SA. We have shown that fibrosis is localized around secondary lymphoid follicles and that fibroblasts are activated by plasma cells via PDGF/PDGFR signaling in IgG4-SA.

**Keywords:** IgG4-related sialadenitis, plasma cell, fibroblast, PDGF-PDGFR signaling, histological spatial analysis

## INTRODUCTION

IgG4-related disease (IgG4-RD) is characterized by increased serum IgG4 levels and swelling of the organs.<sup>1</sup> The major histological features of IgG4-RD are known to be dense lymphoplasmacytic infiltration with many IgG4-positive plasma cells, storiform fibrosis, and obliterative phlebitis.<sup>2,3</sup> In organs with IgG4-RD, tissue injury is often caused by fibroinflammatory infiltration. Thus, glucocorticoids have been used to induce remission in patients with IgG4-RD.<sup>4</sup>

The salivary glands are frequently affected in IgG4-RD, and this condition is termed IgG4-related sialadenitis (IgG4-SA).<sup>5</sup> The main clinical feature of IgG4-SA is bilateral and painless swelling of the salivary glands, especially the submandibular glands.<sup>6</sup> The histological features of

IgG4-SA include lymphoplasmacytic infiltration, the formation of numerous secondary lymph follicles, and dense fibrosis.<sup>6</sup> An increased number of secondary lymph follicles is one of the characteristics of IgG4-SA.<sup>7</sup>

B-cells and plasma cells have been shown to be involved in fibrosis in IgG4-RD<sup>8,9</sup> because rituximab, which targets B-cells, has been reported to reduce the infiltration of inflammatory cells and fibrosis.<sup>10</sup> Secondary lymphoid follicles play a role in the differentiation of B-cells into plasma cells,<sup>11</sup> which have been reported to be involved in fibrosis.<sup>12,13</sup> Therefore, we focused on the formation of many secondary lymphoid follicles and the mechanism underlying this fibrosis in IgG4-SA. We hypothesized that plasma cells are involved in the development of fibrosis in IgG4-SA. In this study, we examined the molecular mechanism underlying the cellular interactions between fibroblasts and plasma cells during


Received: July 8, 2024. Revised: July 30, 2024. Accepted: August 1, 2024. Online Published: September 28, 2024

DOI: 10.3960/jslrt.24040

<sup>1)</sup>Department of Pathology, Yamagata University Faculty of Medicine, Yamagata, Japan, <sup>2)</sup>Department of Otolaryngology, Head and Neck Surgery, Yamagata University Faculty of Medicine, Yamagata, Japan, <sup>3)</sup>Department of Dentistry, Oral and Maxillofacial-Plastic and Reconstructive Surgery, Yamagata University Faculty of Medicine, Yamagata, Japan

**Corresponding author:** Rintaro Ohe, M.D., Ph.D., Department of Pathology, Yamagata University Faculty of Medicine, 2-2-2 Iida-Nishi, Yamagata 990-9585, Japan. E-mail: r-ooe@med.id.yamagata-u.ac.jp

Copyright © 2024 The Japanese Society for Lymphoreticular Tissue Research

 This work is licensed under a Creative Commons Attribution-NonCommercial-ShareAlike 4.0 International License.

fibrosis in IgG4-SA by focusing on collagen type, fibroblast localization, and inflammatory cell infiltration. We used chronic sialadenitis (chronic-SA) due to salivary stones as the control disease for IgG4-SA because chronic-SA is the most common inflammatory disease of the salivary glands.<sup>14</sup>

## MATERIAL AND METHODS

### Patients and tissue specimens

Twelve tissue samples from 12 patients with IgG4-SA were collected after diagnosis at Yamagata University Hospital between 2010 and 2021. The 2020 revised comprehensive diagnostic criteria for IgG4-RD were used to diagnose IgG4-SA in our study.<sup>15</sup> Small samples or samples with little fibrosis were excluded. Finally, we could use three IgG4-SA samples, including two samples with severe collagen deposition (Fig. S1a and b) and one sample with moderate collagen deposition (Fig. S1c). The number of IgG4<sup>+</sup> cells in IgG4-SA in the three cases was 134, 97, and 57 cells/HPF, respectively, and IgG4<sup>+</sup>/IgG<sup>+</sup> plasma cell ratio was 69.7, 64.1, and 69.9, respectively. As controls for IgG4-SA, three tissue samples from three patients with chronic-SA were used, following a previous report.<sup>3</sup> Chronic-SA was synonymous with sialolithiasis. All samples were from the submandibular glands. The tissues were fixed with 10% neutral-buffered formalin for 48 hours at room temperature and embedded in paraffin. Three-micrometer sections were prepared for hematoxylin-eosin (HE) staining, Azan staining, silver staining, and immunohistochemistry (IHC). This study was approved by the Research Ethics Committee of Yamagata University Faculty of Medicine (2020-142) and was performed in accordance with the Declaration of Helsinki.

### Special Stains

Azan staining was used to identify collagen fibers composed mainly of type I collagen. Collagen fibers were stained blue in Azan staining. Silver staining was used to identify reticular fibers composed of type III collagen. Reticular fibers were stained black to greenish brown.

### IHC

Single and double immunostaining were performed with BOND RXm (Leica Biosystems, Nussloch, Germany) according to the manufacturer's protocol. Multiplex immunofluorescence (IF) staining was performed using the tyramide signal amplification-based Opal method, with an Opal 4-Color Automation IHC Kit (Akoya Biosciences, Marlborough, MA). Opal reagents (Opal520; FITC, Opal570; TRITC) were used instead of DAB IHC reagents. The sections were counterstained with spectral DAPI. Multiplex staining was evaluated with an all-in-one fluorescence microscope (BZ-X810, Keyence, Osaka, Japan). Primary antibodies against the following factors were used for IHC: fibroblast activation protein (FAP) (EPR20021, Abcam, Cambridge, UK), multiple myeloma oncogene 1 (MUM1) (MUM1p, DAKO, Glostrup, Denmark), CD163 (10D6, Leica Biosystems), CD204 (SRA-E5, TRANS

GENIC, Hokkaido, Japan), CD206 (5C11, Abnova, Taipei, Taiwan), platelet-derived growth factor (PDGF)  $\beta$  (MM0014-5F66, Abcam), PDGF receptor (PDGFR)  $\beta$  (28E1, Cell Signaling Technology, Danvers, MA), and phosphorylated signal transducer and activator of transcription-3 (pSTAT3) (D3A7, Cell Signaling Technology). Immunohistochemical staining for FAP, MUM1, CD163, and Foxp3 was performed on individual serial sections from formalin-fixed, paraffin-embedded tissue blocks (FFPE) of samples from IgG4-SA patients and chronic-SA patients. MUM1 has been reported to be expressed in plasmablasts and plasma cells in normal tissues.<sup>16</sup> Since MUM1 could be used to detect plasma cells in IgG4-SA and in chronic-SA, we considered MUM1 a suitable marker for plasma cells. Immunohistochemical staining for CD163, CD204, and CD206 was performed on individual serial sections from FFPE tissue from IgG4-SA patients and chronic-SA patients. Double immunostaining for MUM1 and PDGF $\beta$  was performed to evaluate plasma cell-produced PDGF $\beta$ , and double immunostaining for FAP and PDGFR $\beta$  was performed to evaluate fibroblast-expressed PDGFR $\beta$ . Similarly, double immunostaining for FAP and pSTAT3 was performed to evaluate the activation of the PDGF/PDGFR signaling pathway in fibroblasts. To evaluate PDGFR $\beta$  expression in FAP<sup>+</sup> fibroblasts, the fluorescence microscope was used to capture ten high-power fields for each sample, and HALO was used to determine the number of FAP<sup>+</sup> cells and the number of FAP-PDGFR $\beta$  co-expressing cells in each field.

### Evaluation of the area of collagen fibers and the numbers of fibroblasts, plasma cells, macrophages, and Tregs

All slides were converted to digital whole-slide images by Nanozoomer (Hamamatsu Photonics K.K., Shizuoka, Japan). For quantitative analysis, ten analysis regions with a size of 0.237 mm<sup>2</sup> were randomly selected around the secondary lymph follicles and around the dilated ducts in each sample. Histological image analyses were performed with HALO software (Indica Labs, Corrales, NM). HALO measured the area of fibers that were stained blue in the analysis regions of Azan-stained specimens to quantify collagen fibers. For the quantitative analysis of IHC specimens, HALO detected all IHC-positive cells stained with DAB on each slide, such as cells expressing FAP, MUM1, CD163, CD204, CD206, and Foxp3.

### Evaluation of plasma cell–fibroblast interactions using histological spatial analysis

To evaluate cell-to-cell interactions, HALO examined the density of IHC-positive cells and the proximity of one cell to another, as previously reported.<sup>17,18</sup> For example, HALO allocated FAP<sup>+</sup> cells and MUM1<sup>+</sup> cells to yellow triangles and green circles, respectively. The yellow triangles and green circles were synchronized in one chart. The number of MUM1<sup>+</sup> cells was counted every ten  $\mu$ m from a single FAP<sup>+</sup> fibroblast up to 100  $\mu$ m. The calculated number of MUM1<sup>+</sup> cells was corrected according to the area of each analysis because the area of the region analyzed per ten  $\mu$ m depended on the distance from FAP<sup>+</sup> fibroblasts.

## Statistical analysis

Statistical analyses were performed using JMP Pro 16.1.0 (SAS Institute, Cary, NC). The  $\chi^2$  test, Fisher's exact test, or the Mann–Whitney test was used for comparisons between two groups. Differences with  $P$  values  $< 0.05$  were considered significant.

## RESULTS

### Fibrosis was localized around secondary lymphoid follicles in IgG4-SA

In the IgG4-SA group, many secondary lymphoid follicles with germinal centers were found (Fig. 1a), and these lymphoid follicles were large and irregularly shaped (Fig. 1a). Eosinophilic fibers developed around secondary lymphoid follicles, as shown by high magnification (Fig. 1b). These fibers showed blue in Azan staining (Fig. 1c), suggesting that they were collagen fibers. Our results indicated that many collagen fibers developed around secondary lymphoid follicles in IgG4-SA.

In the chronic-SA group, few secondary lymphoid follicles were found (Fig. 1d), and these lymphoid follicles were smaller and rounder (Fig. 1e) than those in IgG4-SA samples. Few eosinophilic fibers developed around secondary lymphoid follicles, as shown by high magnification (Fig. 1e). These few fibers showed blue in Azan staining (Fig. 1f). Our results suggested that few collagen fibers developed around secondary lymphoid follicles. Quantitative analysis of collagen fibers by Azan staining revealed that the area of collagen fibers in the IgG4-SA group was significantly larger than that in the chronic-SA group ( $P < 0.001$ ; Fig. 1g).

In the IgG4-SA group, few eosinophilic fibers developed around the ducts (Fig. S2a). These fibers showed blue in Azan staining (Fig. S2b). Few collagen fibers developed around the ducts in the IgG4-SA group. In the chronic-SA group, eosinophilic fibers developed around the dilated ducts (Fig. S2c). These fibers showed blue in Azan staining (Fig. S2d). Many collagen fibers developed around the dilated ducts in chronic-SA. In the IgG4-SA group, fibrosis was mainly observed around secondary lymphoid follicles. In the chronic-SA group, fibrosis was mainly observed around the dilated ducts.

### Localization of collagen fibers, reticular fibers, and fibroblasts around secondary lymphoid follicles in IgG4-SA

We examined the collagen type associated with fibrosis in IgG4-SA because fibroblasts produce various types of collagens (Fig. 2). We identified collagen fibers composed mainly of type I collagen with Azan staining and reticular fibers composed of type III collagen with silver staining. Azan staining revealed fewer collagen fibers near secondary lymphoid follicles and more collagen fibers away from secondary lymphoid follicles (Fig. 2a). Detailed observation by Azan staining revealed sparse collagen fibers near secondary

lymphoid follicles (Fig. 2b) and dense collagen fibers away from secondary lymphoid follicles (Fig. 2c). Silver staining revealed dense reticular fibers near secondary lymphoid follicles (Fig. 2d) and sparse reticular fibers away from secondary lymphoid follicles (Fig. 2e). FAP staining revealed many positive fibroblasts near secondary lymphoid follicles (Fig. 2f) and few positive fibroblasts away from secondary lymphoid follicles (Fig. 2g). The numbers of FAP<sup>+</sup> fibroblasts around secondary lymphoid follicles in IgG4-SA samples were significantly higher than those in chronic-SA samples ( $P < 0.001$ ; Fig. 2h).

### Comparison of the number of inflammatory cells in fibrotic regions in the IgG4-SA and chronic-SA groups

IHC-MUM1 was used to identify plasma cells associated with fibrosis in IgG4-SA samples. Many MUM<sup>+</sup> plasma cells infiltrated in the fibrotic regions around secondary lymphoid follicles in IgG4-SA samples (Fig. 3a). Few plasma cells infiltrated in the fibrotic regions around the dilated ducts in chronic-SA samples (Fig. 3b). Quantitative analysis revealed that the ratio of plasma cells to FAP<sup>+</sup> fibroblasts in the fibrotic regions around secondary lymphoid follicles in the IgG4-SA group was significantly higher than that in the fibrotic regions around the dilated ducts in the chronic-SA group ( $P < 0.001$ ; Fig. 3c). These results indicated that plasma cells were involved in the induction of fibrosis in IgG4-SA. Similarly, immunohistochemical analysis of CD163, CD204, and CD206 was used to identify M2 macrophages, and Foxp3-IHC was used to identify Tregs. Quantitative analysis revealed that the ratio of CD163<sup>+</sup> M2 macrophages to fibroblasts in IgG4-SA samples was similar to that in chronic-SA samples ( $P = 0.712$ ; Fig. 3d). The actual numbers of CD163<sup>+</sup> M2 macrophages and CD204<sup>+</sup> M2 macrophages in IgG4-SA samples were significantly higher than those in chronic-SA samples (data not shown). The ratio of Tregs to fibroblasts in the IgG4-SA group was slightly higher than that in the chronic-SA group, and this difference was significant ( $P < 0.001$ ; Fig. 3e). The number of these inflammatory cells tended to increase in the two cases with severe collagen deposition than in one case with moderate collagen deposition (data not shown).

### Histological spatial analysis of fibroblasts and plasma cells in the fibrotic region in IgG4-SA

If plasma cells were involved in the activation of fibroblasts in IgG4-SA, many plasma cells would be expected to be localized near fibroblasts. Histological spatial analysis was used to examine the number of plasma cells and the distance between plasma cells and fibroblasts. FAP<sup>+</sup> fibroblasts were observed near secondary lymphoid follicles (Fig. 4a). FAP<sup>+</sup> fibroblasts were allocated yellow triangles by HALO (Fig. 4b) and plotted on a grid chart (Fig. 4c). MUM1<sup>+</sup> plasma cells were observed in the identical region in the serial FAP-IHC specimen (Fig. 4d). MUM1<sup>+</sup> plasma cells were allocated green circles by HALO (Fig. 4e) and plotted on a grid chart (Fig. 4f). The yellow triangles in Fig. 4c and the green circles in Fig. 4f were synchronized into one grid



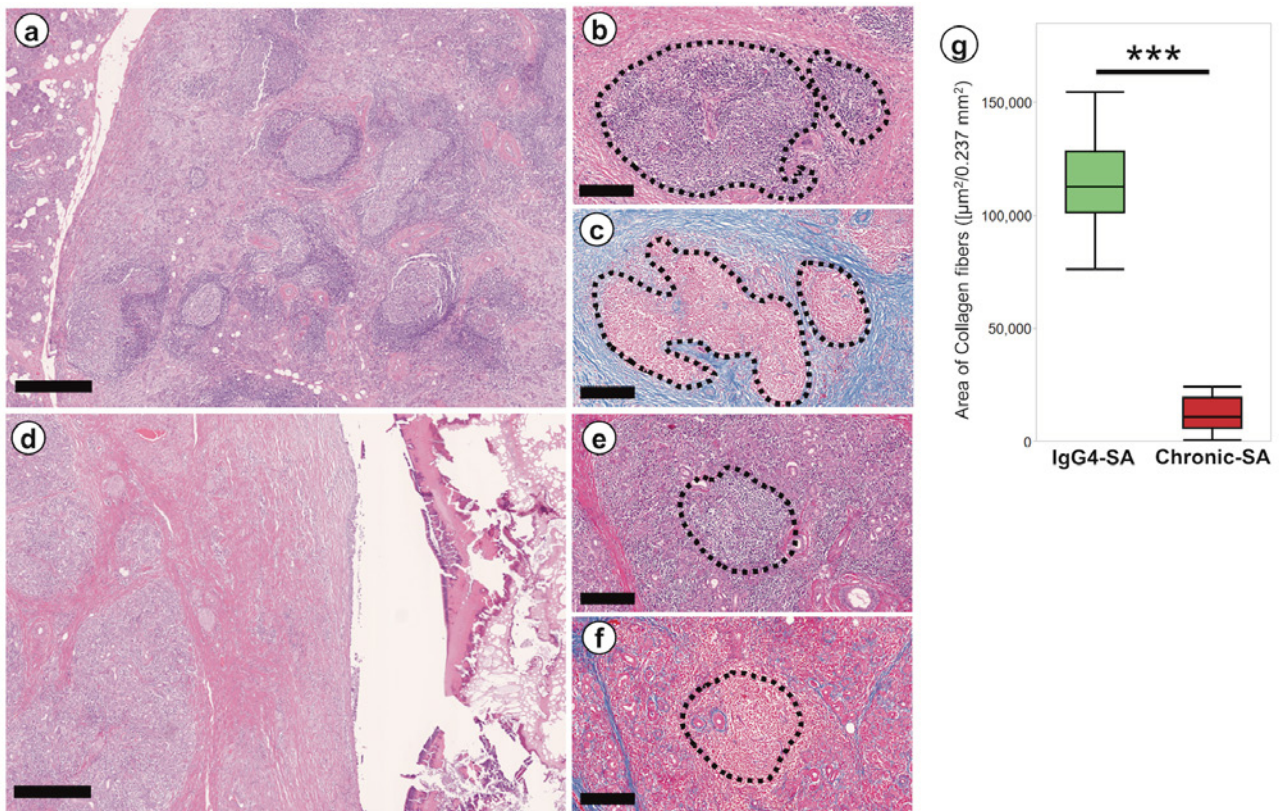


**Fig. 1.** Fibrosis was localized around the secondary lymphoid follicles in IgG4-related sialadenitis  
*a:* Low-power field image of the IgG4-related sialadenitis (IgG4-SA) sample. *b:* High-power field image of the IgG4-SA sample. *c:* Collagen fibers developed around the secondary lymphoid follicles. *d:* Low-power field image of the chronic sialadenitis (chronic-SA) sample. *e:* High-power field image of the acinar area in the chronic-SA sample. *f:* A few collagen fibers were observed around the secondary lymphoid follicles. *g:* The area of collagen fibers around secondary lymphoid follicles in the IgG4-SA group was significantly larger than that in the chronic-SA group. The area closed by the dashed line showed lymphoid follicles (*b, c, e, and f*). Scale bars, 500  $\mu\text{m}$  (*a and d*) and 250  $\mu\text{m}$  (*b, c, e, and f*). **\*\*\***,  $P < 0.001$ .

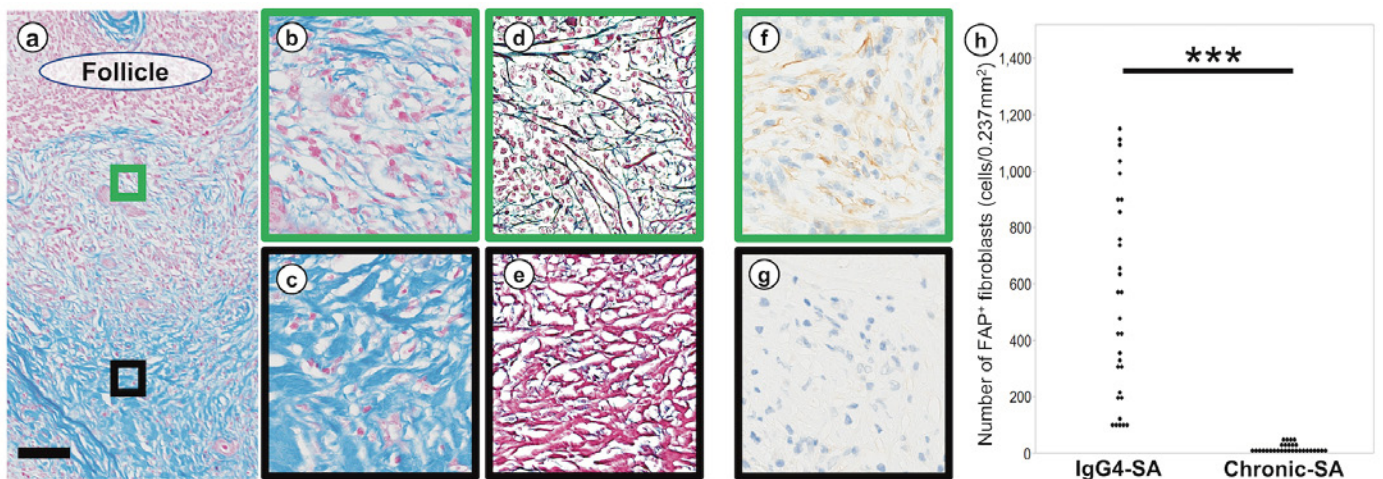


**Fig. 2.** Localization of collagen fibers, reticular fibers, and fibroblasts  
*a:* Localization of fibrosis around secondary lymph follicle. The green rectangle was set near the secondary lymphoid follicle, and the black rectangle was set away from the secondary lymphoid follicle. *b:* Collagen fibers were sparse near the secondary lymph follicles. *c:* Collagen fibers were dense away from the secondary lymphoid follicles. *d:* Reticular fibers developed near the secondary lymphoid follicles. *e:* Collagen fibers in red were predominant away from the secondary lymphoid follicles. *f:* Many FAP<sup>+</sup> fibroblasts were observed near the secondary lymphoid follicles. *g:* Few FAP<sup>+</sup> fibroblasts were observed away from the secondary lymphoid follicles. *h:* The number of FAP<sup>+</sup> fibroblasts around the secondary lymphoid follicles in IgG4-related sialadenitis (IgG4-SA) group was significantly higher than in chronic sialadenitis (chronic-SA) group. *a, b, and c* were Azan staining; *d and e* were silver staining; *g and h* were immunohistochemistry of FAP. Scale bars, 500  $\mu\text{m}$ . **\*\*\***,  $P < 0.001$ .

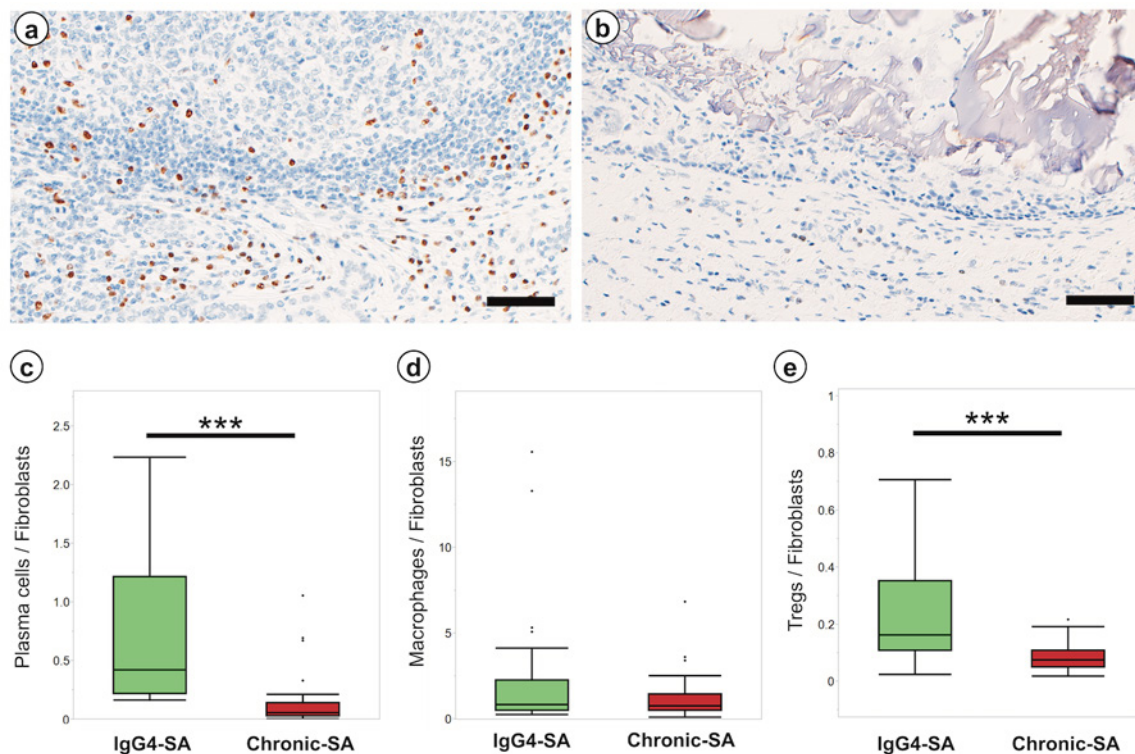


**Fig. 3.** Inflammatory cells in fibrotic regions of IgG4-related sialadenitis and chronic sialadenitis **a:** Many MUM1<sup>+</sup> cells were observed around the secondary lymphoid follicles in IgG4-related sialadenitis (IgG4-SA). **b:** Only a few MUM1<sup>+</sup> cells were observed around the dilated ducts in chronic sialadenitis (chronic-SA). **c, d, and e:** The number of plasma cells (**c**), macrophages (**d**), and Tregs (**e**) per a fibroblast was compared around the secondary lymphoid follicles in IgG4-SA and dilated ducts in chronic-SA. Scale bar, 100  $\mu$ m. \*\*\*,  $P < 0.001$ .

chart (Fig. 4g). The number of MUM1<sup>+</sup> plasma cells was measured every ten  $\mu$ m from a single fibroblast up to 100  $\mu$ m (Fig. 4h). The histogram revealed that 90.4% of MUM1<sup>+</sup> plasma cells accumulated within 20  $\mu$ m of FAP<sup>+</sup> fibroblasts (Fig. 4i). These results suggested an interaction between plasma cells and fibroblasts in the fibrotic region around secondary lymphoid follicles in IgG4-SA.

#### Identification of PDGF expression in plasma cells and PDGFR expression in fibroblasts

Because the interaction between plasma cells and fibroblasts was expected to be cytokine-mediated, we examined whether the PDGF/PDGFR signaling pathway was involved. MUM1<sup>+</sup> plasma cells were labeled with TRITC (red) (Fig. 5a), PDGF $\beta$ <sup>+</sup> cells were labeled with FITC (green) (Fig. 5b), and the nuclei were stained with DAPI (blue) (Fig. 5c) in a multiple immunofluorescence assay. The merged image showed nuclei stained with TRITC (red) and cytoplasm stained with FITC (green) (Fig. 5d). This merged image indicated that MUM1<sup>+</sup> plasma cells expressed PDGF $\beta$  (Fig. 5d). FAP<sup>+</sup> fibroblasts were labeled with FITC (green) (Fig. 5e), PDGF $\beta$ <sup>+</sup> cells were labeled with TRITC (red) (Fig. 5f), and the nuclei were stained with DAPI (blue) (Fig. 5g). The merged image showed cells with yellow cytoplasm (Fig. 5h). This merged image indicated that FAP<sup>+</sup> fibroblasts expressed PDGF $\beta$  (Fig. 5h). The PDGF $\beta$  expression rate in FAP<sup>+</sup> fibroblasts in IgG4-SA samples were not significantly differ-

ent from that in chronic-SA samples (Fig. S3). The expression of pSTAT3 was examined in fibroblasts to confirm PDGF/PDGFR signal transduction because pSTAT3 is one of the downstream molecules of PDGF/PDGFR signaling. FAP<sup>+</sup> fibroblasts were labeled with FITC (green) (Fig. 5i), pSTAT3<sup>+</sup> cells were labeled with TRITC (red) (Fig. 5j), and the nuclei were stained with DAPI (blue) (Fig. 5k). The merged image showed that the cytoplasm was stained with FITC (green) and that the nucleus was stained with TRITC (red) (Fig. 5l). This merged image indicated that FAP<sup>+</sup> fibroblasts expressed pSTAT3 (Fig. 5l). Although PDGF promotes vascular growth, our observations of HE and Azan-stained specimens of the IgG4-SA group showed no marked vascular growth in the infiltrated areas of MUM1<sup>+</sup>PDGF $\beta$ <sup>+</sup> plasma cells.

## DISCUSSION

IgG4-RD, which includes IgG4-SA, is characterized by dense lymphoplasmacytic infiltration and marked fibrosis.<sup>1,2</sup> The histological characteristics of IgG4-SA include the formation of secondary lymphoid follicles and dense collagen deposition with storiform fibrosis.<sup>6</sup> Our data showed that collagen fibers were identified around secondary lymphoid follicles in the IgG4-SA group. The histological characteristics of chronic-SA include fibrosis in periductal and intralobular areas.<sup>19</sup> Our data showed that collagen fibers were iden-



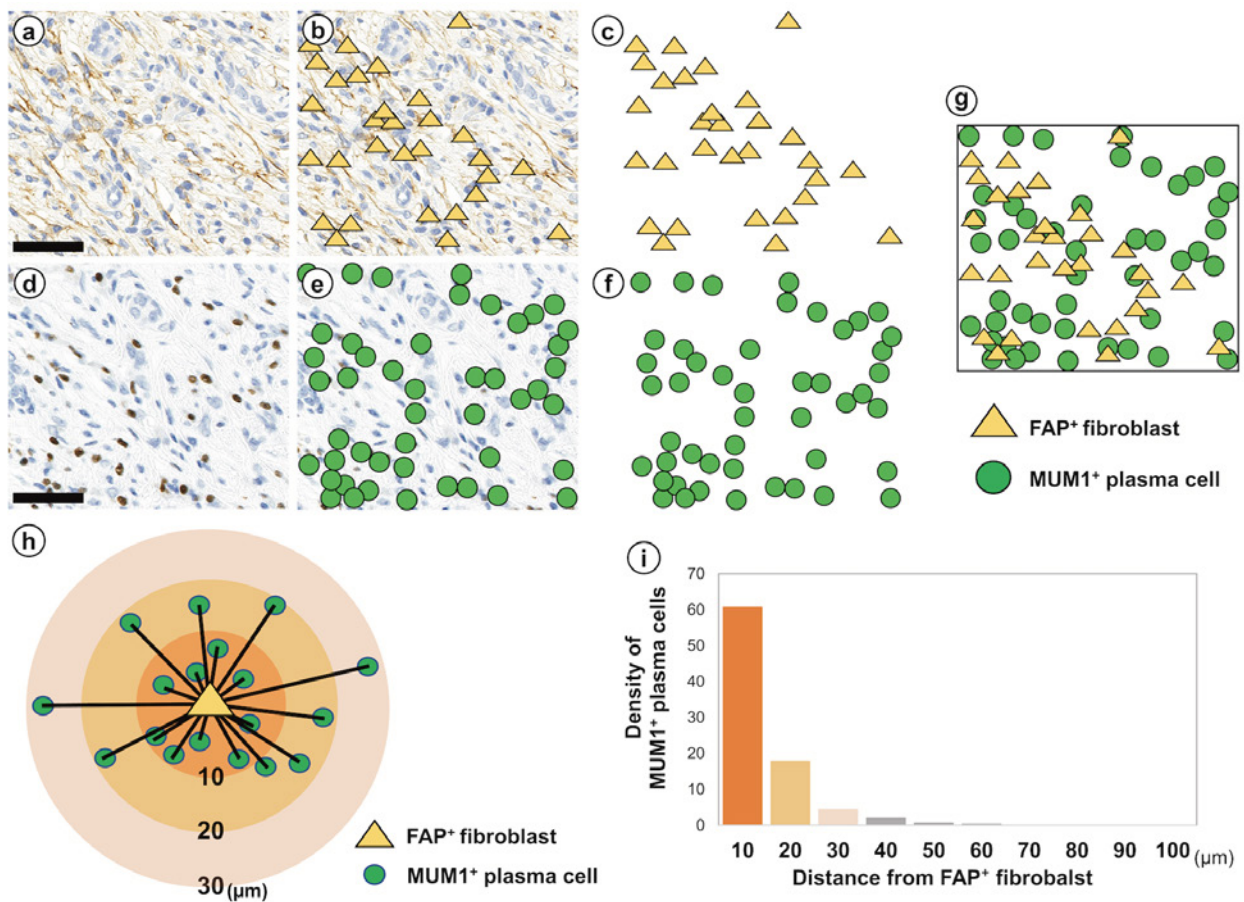


**Fig. 4.** Histological spatial analysis of fibroblasts and plasma cells in IgG4-related sialadenitis. FAP<sup>+</sup> fibroblasts in the fibrotic region around secondary lymphoid follicles in IgG4-related sialadenitis (IgG4-SA) were recognized by image analysis software (a) and allocated yellow triangles (b). Yellow triangles were plotted on the grid chart (c). MUM1<sup>+</sup> plasma cells at the same location as the FAP-immunohistochemistry specimen were recognized by image analysis software (d) and allocated green circles (e). Green circles were plotted on the grid chart (f). Yellow triangles (c) and green circles (f) were synchronized and overlaid into one grid chart (g). The schematic diagram (h) shows the distribution of MUM1<sup>+</sup> plasma cells around a fibroblast. The histogram (i) shows the density of MUM1<sup>+</sup> cells at each distance from the fibroblasts. Approximately 90% of the plasma cells were present within 20 μm of the fibroblasts. Scale bars, 50 μm.

tified around dilated ducts in chronic-SA samples, and fewer collagen fibers were observed around secondary lymphoid follicles in chronic-SA samples. Taken together, we believe that fibrosis localized around secondary lymph follicles is one of the characteristics of IgG4-SA.

Next, we examined the type of collagen in fibrosis of IgG4-SA. Type III collagen, which makes up reticular fibers, was abundant near secondary lymphoid follicles in the IgG4-SA group. Because type III collagen is known to be induced during the early stage of fibrosis in the wound healing process,<sup>20</sup> fibrosis with abundant type III collagen near secondary lymphoid follicles corresponded to fibrosis associated with the early stage of wound healing in this study. Type I collagen, which mainly makes up collagen fibers, was abundant away from secondary lymphoid follicles. Because type I collagen is known to be induced during the late stage of fibrosis in the wound healing process,<sup>20,21</sup> abundant type I collagen fibrosis observed away from secondary lymphoid follicles corresponded to fibrosis associated with the late stage of wound healing. Our study revealed that many acti-

vated fibroblasts were near secondary lymphoid follicles and that fewer activated fibroblasts were located away from secondary lymphoid follicles. Fibroblasts are known to be induced in the early stage of fibrosis during wound healing but are removed by apoptosis during the late stage.<sup>20,22</sup> Our data suggested that the presence of many activated fibroblasts near secondary lymphoid follicles corresponded to fibrosis associated with the early stage of wound healing.<sup>20,22</sup> Few activated fibroblasts away from secondary lymphoid follicles corresponded to fibrosis associated with the late stage of wound healing.<sup>20,22</sup> Based on the distributions of type III collagen, type I collagen, and activated fibroblasts, fibrosis near secondary lymphoid follicles corresponded to fibrosis associated with the early stage of wound healing, and fibrosis away from secondary lymphoid follicles corresponded to fibrosis associated with the late stage of wound healing.<sup>20-22</sup> In summary, in IgG4-SA, fibrosis near secondary lymph follicles corresponds to fibrosis during the early stage of wound healing, and fibrosis away from secondary lymphoid follicles corresponds to the late stage of wound healing.

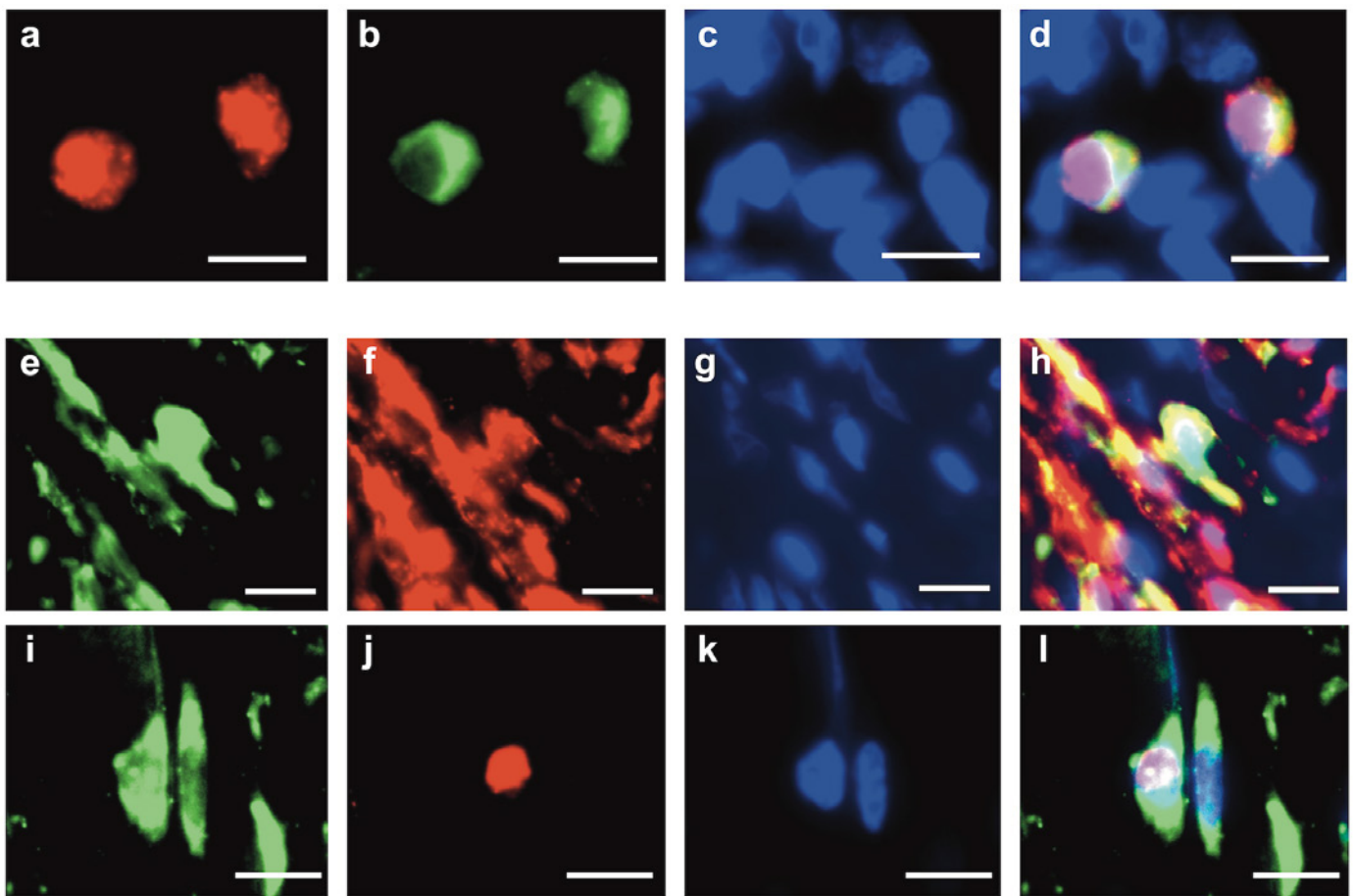


**Fig. 5.** Identification of platelet-derived growth factor  $\beta$  expression in plasma cells and platelet-derived growth factor  $\beta$  receptor expression in fibroblasts by multiple immunofluorescence assay

**a:** Multiplex immunofluorescence (IF) staining of MUM1. MUM1<sup>+</sup> cells were stained with TRITC (red). **b:** Multiplex IF staining of platelet-derived growth factor (PDGF) $\beta$ . PDGF $\beta$ <sup>+</sup> cells were stained with FITC (green). **c:** DAPI staining. **d:** Merged image of **a**, **b**, and **c**. **e:** Multiplex IF staining of FAP. FAP<sup>+</sup> cells were stained with FITC (green). **f:** Multiplex IF staining of PDGF receptor (PDGFR) $\beta$ . PDGFR $\beta$ <sup>+</sup> cells were stained with TRITC (red). **g:** DAPI staining. **h:** Merged image of **e**, **f**, and **g**. **i:** Multiplex IF staining of FAP. FAP<sup>+</sup> cells were stained with FITC (green). **j:** Multiplex IF staining of phosphorylated signal transducer and activator of transcription-3 (pSTAT3). pSTAT3<sup>+</sup> cells were stained with TRITC (red). **k:** DAPI staining. **l:** Merged image of **i**, **j**, and **k**.

Several reports have demonstrated that plasma cells are involved in the activation of fibroblasts.<sup>23</sup> In this study, we used the anti-MUM1 antibody as a plasma cell marker and compared the number of plasma cells in IgG4-SA patients with that in chronic-SA patients. We found that the number of MUM1<sup>+</sup> plasma cells in the IgG4-SA group was significantly higher than that in the chronic-SA group. Plasmablasts and plasma cells have been reported to activate fibroblasts in IgG4-SA and IgG4-related pancreatitis.<sup>24</sup> These results suggested that MUM1<sup>+</sup> plasma cells were involved in the activation of fibroblasts in IgG4-SA.

Several reports have demonstrated that inflammatory cells, such as M2 macrophages<sup>25,26</sup> and Tregs,<sup>27,28</sup> are involved in the activation of fibroblasts. M2 macrophages are known to play essential roles in tissue repair and the progression of fibrotic disease.<sup>29,30</sup> During the wound healing process, M2 macrophages are mainly involved in the activation of fibroblasts.<sup>30</sup> In IgG4-RD, which includes IgG4-SA, M2 macrophages have been reported to promote fibrosis.<sup>26</sup> In this study, the number of CD163<sup>+</sup> M2 macrophages per a fibro-

blast in the IgG4-SA group was similar to that in the chronic-SA group. Our results suggested that M2 macrophages contributed to fibrosis in both IgG4 and chronic-SA. Because the induction of macrophages in chronic-SA was associated with the destruction of ducts and glands,<sup>19</sup> we expected the number of M2 macrophages in the chronic-SA group to be higher than that in the IgG4-SA group.

Tregs are known to suppress excessive immune responses and to promote wound healing.<sup>27,31</sup> The number of Tregs has been reported to increase in IgG4-RD,<sup>32</sup> and Tregs have been reported to be involved in fibrosis in IgG4-RD.<sup>33</sup> In this study, the number of Tregs in IgG4-SA patients was significantly higher than that in chronic-SA patients. Our data suggested that Tregs were involved in fibrosis in IgG4-SA. Taken together, MUM1<sup>+</sup> plasma cells would be involved in IgG4-SA, M2 macrophages would contribute to fibrosis in both IgG4-SA and chronic-SA, and Tregs may contribute to fibrosis in IgG4-SA. The contribution of Tregs to fibrosis was presumed to be limited because the number of plasma cells and M2 macrophages in the IgG4-SA group was higher

than the number of Tregs. Overall, we believe that the involvement of plasma cells in the activation of fibroblasts is one of the characteristics of IgG4-SA.

Fibroblasts are known to be activated by cytokine-mediated paracrine signaling after cytokine secretion from inflammatory cells.<sup>34</sup> When inflammatory cells produce cytokines to activate fibroblasts, a high density of cytokines would be required to activate fibroblasts. Inflammatory cells are thought to accumulate near a single fibroblast during paracrine signaling. In this study, we hypothesized that many plasma cells accumulated near a single fibroblast in IgG4-SA. Our histological spatial analysis revealed that 90.4% of the plasma cells accumulated within 20  $\mu\text{m}$  of fibroblasts. Because the size of a plasma cell is approximately 9–12  $\mu\text{m}$ ,<sup>35</sup> a distance of 20  $\mu\text{m}$  is comparable to the size of two plasma cells. These results suggest that fibroblasts would be activated by plasma cells through cytokine-mediated paracrine signaling.

PDGF/PDGFR signaling is one of the central mediators of fibrosis.<sup>36</sup> Because fibroblasts have been reported to be activated by plasma cells via PDGF in IgG4-RD,<sup>24</sup> we focused on PDGF/PDGFR signaling. We examined PDGFR $\beta$  expression in MUM1<sup>+</sup> plasma cells in the IgG4-SA group, and the results suggested that MUM1<sup>+</sup> plasma cells produced PDGF $\beta$ . We found that FAP<sup>+</sup> fibroblasts expressed PDGFR $\beta$  and pSTAT3. STAT3 is known to be one of the downstream molecules of PDGF/PDGFR signaling,<sup>37</sup> and PDGF/PDGFR signaling has been reported to be involved in the upregulation of STAT3 expression in fibroblasts.<sup>38,39</sup> Fibroblasts would be directly activated by MUM1<sup>+</sup> plasma cells through PDGF/PDGFR signaling. Because the PDGFR $\beta$  expression rate in fibroblasts in the IgG4-SA group was similar to that in the chronic-SA group, we found that the characteristics of fibroblasts in IgG4-SA samples were similar to those of fibroblasts in chronic-SA samples. Since many MUM1<sup>+</sup> plasma cells were localized around secondary lymphoid follicles in IgG4-SA samples, PDGF produced by plasma cells may play an important role in fibrosis around secondary lymphoid follicles in IgG4-SA.

We acknowledge several limitations in this study. Because we only investigated three patients with IgG4-SA, future studies should examine a larger sample size. The small sample size did not allow for evaluation of the fibrosis formation process over time. Since inflammatory cell infiltration tended to be more severe in IgG4-SA samples with severe fibrosis in this study, we would like to increase our sample size in the future to investigate association between the degree of inflammation and fibrosis progression. In addition, our study samples were limited to FFPE, and more studies are needed to elucidate the detailed interaction between plasma cells and fibroblasts. More specifically, since PDGF $\beta$ <sup>+</sup> plasma cells are expected to interact with PDGFR $\beta$ <sup>+</sup> fibroblasts, we would like to study in the future the activation of fibroblasts by PDGF $\beta$ <sup>+</sup> plasma cells *in vitro* and the spatial interaction between PDGF $\beta$ <sup>+</sup> plasma cells and PDGFR $\beta$ <sup>+</sup> fibroblasts by quintuple fluorescent staining.

In conclusion, fibrosis in IgG4-SA was localized around

secondary lymphoid follicles, and fibroblasts were activated by plasma cells through PDGF/PDGFR signaling.

## ACKNOWLEDGMENTS

We are grateful to Mr. Toshinori Suzuki, Mr. Tomonori Saito, Mr. Teppei Shiraiwa, Ms. Ami Shida, Ms. Ayumi Suzuki, Ms. Hiromi Murata, and Ms. Junko Takeda for pathological technical assistance in this study. I would like to thank AJE (<https://www.aje.com/jp/>) for the English language review. This work was supported by JSPS KAKENHI Grant numbers JP24K10326, JP23K06646, JP22K09661, and JP21K06901.

## AUTHOR CONTRIBUTIONS

Takumi Kitaoka performed the experiments, analyzed the stained samples, and wrote the paper. Rintaro Ohe designed the experiments and co-wrote the paper. Takano Kabasawa, Masayuki Kaneko, Nobuyuki Sasahara, Michihisa Kono, Kazushi Suzuki, Naoya Uchiyama, Rinako Ogawa assisted in the experimental process. Mitsuru Futakuchi supervised the study. All authors contributed to the discussion and revision of the manuscript and have approved the final version.

## CONFLICT OF INTEREST

The authors have no competing interests to declare that are relevant to the content of this article.

## REFERENCES

- 1 Satou A, Notohara K, Zen Y, *et al.* Clinicopathological differential diagnosis of IgG4-related disease: A historical overview and a proposal of the criteria for excluding mimickers of IgG4-related disease. *Pathol Int.* 2020; 70: 391-402.
- 2 Deshpande V, Zen Y, Chan JK, *et al.* Consensus statement on the pathology of IgG4-related disease. *Mod Pathol.* 2012; 25: 1181-1192.
- 3 Gion Y, Takeuchi M, Shibata R, *et al.* Up-regulation of activation-induced cytidine deaminase and its strong expression in extra-germinal centres in IgG4-related disease. *Sci Rep.* 2019; 9: 761.
- 4 Katz G, Stone JH. Clinical Perspectives on IgG4-Related Disease and Its Classification. *Annu Rev Med.* 2022; 73: 545-562.
- 5 Kamisawa T, Zen Y, Pillai S, Stone JH. IgG4-related disease. *Lancet.* 2015; 385: 1460-1471.
- 6 Fragoulis GE, Zampeli E, Moutsopoulos HM. IgG4-related sialadenitis and Sjögren's syndrome. *Oral Dis.* 2017; 23: 152-156.
- 7 Zen Y, Nakanuma Y. IgG4-related disease: a cross-sectional study of 114 cases. *Am J Surg Pathol.* 2010; 34: 1812-1819.
- 8 Puxeddu I, Capocchi R, Carta F, *et al.* Salivary Gland Pathology in IgG4-Related Disease: A Comprehensive Review. *J Immunol Res.* 2018; 2018: 6936727.



- 9 Chen LYC, Mattman A, Seidman MA, Carruthers MN. IgG4-related disease: what a hematologist needs to know. *Haematologica*. 2019; 104: 444-455.
- 10 Della-Torre E, Feeney E, Deshpande V, *et al*. B-cell depletion attenuates serological biomarkers of fibrosis and myofibroblast activation in IgG4-related disease. *Ann Rheum Dis*. 2015; 74: 2236-2243.
- 11 Jaffe ES, Campo E, Harris NL, *et al*. Introduction and overview of the classification of lymphoid neoplasms. In: Swerdlow SH, Campo E, Harris NL, *et al*. (ed): WHO classification of tumours of haematopoietic and lymphoid tissues. Revised 4 ed., Lyon, International Agency for Research on Cancer (IARC). 2017; pp. 190-198.
- 12 Ise W, Kurosaki T. Plasma cell differentiation during the germinal center reaction. *Immunol Rev*. 2019; 288: 64-74.
- 13 Ohe R, Aung NY, Meng H, *et al*. Localization of collagen modifying enzymes on fibroblastic reticular cells and follicular dendritic cells in non-neoplastic and neoplastic lymphoid tissues. *Leuk Lymphoma*. 2016; 57: 1687-1696.
- 14 Li W, Wei L, Wang F, *et al*. An experimental chronic obstructive sialadenitis model by partial ligation of the submandibular duct characterised by sialography, histology, and transmission electron microscopy. *J Oral Rehabil*. 2018; 45: 983-989.
- 15 Umehara H, Okazaki K, Kawa S, *et al*. The 2020 revised comprehensive diagnostic (RCD) criteria for IgG4-RD. *Mod Rheumatol*. 2021; 31: 529-533.
- 16 Hirai A, Aung NY, Ohe R, *et al*. Expression of TRPM8 in human reactive lymphoid tissues and mature B-cell neoplasms. *Oncol Lett*. 2018; 16: 5930-5938.
- 17 Suzuki K, Ohe R, Kabasawa T, *et al*. Histological spatial analysis on the induction of PD-L1<sup>+</sup> macrophages by CD8<sup>+</sup> T cells at the marginal microenvironment of triple-negative breast cancer. *Breast Cancer*. 2023; 30: 1094-1104.
- 18 Kawamura I, Ohe R, Suzuki K, *et al*. Neighboring macrophage-induced alteration in the phenotype of colorectal cancer cells in the tumor budding area. *Cancer Cell Int*. 2024; 24: 107.
- 19 Teymoortash A, Tiemann M, Schrader C, Werner JA. Characterization of lymphoid infiltrates in chronic obstructive sialadenitis associated with sialolithiasis. *J Oral Pathol Med*. 2004; 33: 300-304.
- 20 Boris Hinz GG, Thomas A. Seemayer, and Wlater Schürch: Myofibroblast. Fourth Edition ed, Philadelphia, PA, Lippincott Williams & Wilkins. 2012; pp. 142-143.
- 21 Broughton G II, Janis JE, Attinger CE. The basic science of wound healing. *Plast Reconstr Surg*. 2006; 117: 12S-34S.
- 22 Velnar T, Bailey T, Smrkolj V. The wound healing process: an overview of the cellular and molecular mechanisms. *J Int Med Res*. 2009; 37: 1528-1542.
- 23 Minici C, Rigamonti E, Lanzillotta M, *et al*. B lymphocytes contribute to stromal reaction in pancreatic ductal adenocarcinoma. *OncoImmunology*. 2020; 9: 1794359.
- 24 Della-Torre E, Rigamonti E, Perugino C, *et al*. B lymphocytes directly contribute to tissue fibrosis in patients with IgG4-related disease. *J Allergy Clin Immunol*. 2020; 145: 968-981.e14.
- 25 Hesketh M, Sahin KB, West ZE, Murray RZ. Macrophage Phenotypes Regulate Scar Formation and Chronic Wound Healing. *Int J Mol Sci*. 2017; 18: 1545.
- 26 Chinju A, Moriyama M, Kakizoe-Ishiguro N, *et al*. CD163<sup>+</sup> M2 Macrophages Promote Fibrosis in IgG4-Related Disease Via Toll-like Receptor 7/Interleukin-1 Receptor-Associated Kinase 4/NF-κB Signaling. *Arthritis Rheumatol*. 2022; 74: 892-901.
- 27 Zhang C, Li L, Feng K, *et al*. 'Repair' Treg Cells in Tissue Injury. *Cell Physiol Biochem*. 2017; 43: 2155-2169.
- 28 Kalekar LA, Cohen JN, Prevel N, *et al*. Regulatory T cells in skin are uniquely poised to suppress profibrotic immune responses. *Sci Immunol*. 2019; 4: eaaw2910.
- 29 Sica A, Mantovani A. Macrophage plasticity and polarization: in vivo veritas. *J Clin Invest*. 2012; 122: 787-795.
- 30 Kim SY, Nair MG. Macrophages in wound healing: activation and plasticity. *Immunol Cell Biol*. 2019; 97: 258-267.
- 31 Li J, Tan J, Martino MM, Lui KO. Regulatory T-Cells: Potential Regulator of Tissue Repair and Regeneration. *Front Immunol*. 2018; 9: 585.
- 32 Mahajan VS, Mattoo H, Deshpande V, Pillai SS, Stone JH. IgG4-related disease. *Annu Rev Pathol*. 2014; 9: 315-347.
- 33 Liu C, Zhang P, Zhang W. Immunological mechanism of IgG4-related disease. *J Transl Autoimmun*. 2020; 3: 100047.
- 34 Wynn TA. Cellular and molecular mechanisms of fibrosis. *J Pathol*. 2008; 214: 199-210.
- 35 Sell S, Max EE. Immunology, Immunopathology, and Immunity, ASM Press. 2001; pp. 10-32.
- 36 Klinkhammer BM, Floege J, Boor P. PDGF in organ fibrosis. *Mol Aspects Med*. 2018; 62: 44-62.
- 37 Huynh J, Chand A, Gough D, Ernst M. Therapeutically exploiting STAT3 activity in cancer - using tissue repair as a road map. *Nat Rev Cancer*. 2019; 19: 82-96.
- 38 Jin Y, Ding L, Ding Z, *et al*. Tensile force-induced PDGF-BB/PDGFRβ signals in periodontal ligament fibroblasts activate JAK2/STAT3 for orthodontic tooth movement. *Sci Rep*. 2020; 10: 11269.
- 39 Montero P, Milara J, Roger I, Cortijo J. Role of JAK/STAT in Interstitial Lung Diseases; Molecular and Cellular Mechanisms. *Int J Mol Sci*. 2021; 22: 6211.